ACS OMEGA

http://pubs.acs.org/journal/acsodf

Article

Exploration of Nitroaromatic Antibiotics *via* Sanger's Reagent: Synthesis, *In Silico*, and Antimicrobial Evaluation

Mohammed Salah Ayoup,* Ahmed R. Rabee, Hamida Abdel-Hamid, Marwa F. Harras, Nagwan G. El Menofy, and Magda M. F. Ismail

Cite This: *ACS Omega* 2022, 7, 5254−5263

Read Online

ACCESS | Metrics & More | Article Recommendations | Supporting Information

ABSTRACT: Facile synthesis of molecular hybrids containing a 2,4-dinitrophenyl moiety was achieved *via* nucleophilic aromatic substitution of the fluoride anion of Sanger's reagent (2,4-dinitrofluorobenzene) with various *N*, *S*, and *O* nucleophiles, considered as bioactive moieties. Antimicrobial evaluation of the new hybrids was carried out using amoxicillin and nystatin as antibacterial and antifungal reference standards, respectively. MIC test results identified the compounds **3, 4**, and **7** as the most active hybrids against standard strains and multidrug-resistant strains (MDR) of *Staphylococcus aureus*, *Escherichia coli*, and *Pseudomonas aurginosa*. Most of the hybrids displayed two times the antibacterial activity of AMOX against MDR *Pseudomonas aeruginosa*, *E. coli*, and a standard strain of *P. aeruginosa* (ATCC 29853), while demonstrating a weak antifungal profile against *Candida albicans*. Selectivity profiles of the promising compounds **3, 4, 6, 7, 8**, and **11** on WI-38 human cells were characterized, which indicated that compound **3** is the safest one (CC_{50} 343.72 μM). The preferential anti-Gram-negative activity of our compounds led us to do docking studies on DNA gyrase B. Docking revealed that the potential antimicrobial compounds fit well into the active site of DNA gyrase B. Furthermore, *in silico* absorption, distribution, metabolism, and excretion (ADME) predictions revealed that most of the new compounds have high gastrointestinal absorption and a good oral bioavailability with no BBB permeability.

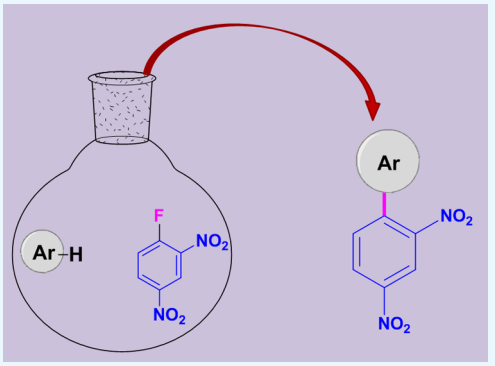

1. INTRODUCTION

Contagious diseases generally occur in tropical and subtropical communities. The virulence of such diseases is competent to multiply in human hosts, justifying their continuous survival. Microbes are progressively modifying and provoking resistant strains to contemporary clinical medicines. The developing antibiotic resistance crisis, due to drug-resistant Gram-positive and Gram-negative bacteria, constitutes urgency for the evolution of improved medications to cure these infections.[1]

Nitroaromatic compounds having one or more nitro functionalities directly bonded to an aromatic group exhibit biological assets, permitting their clinical usage as antibiotics, for instance, metronidazole **I**, niclosamide **II**, chloramphenicol **III**, and tinidazole IV, as shown in Figure 1.[2−5]

Nitroaromatic antibiotics necessitate reductive bioactivation *via* metabolism, converting the NO_2 group to nitric oxide (NO) or reactive nitrogen species (RNS) for antimicrobial activity. This is carried out using nitroreductases (NTRs), which are found almost exclusively in bacteria and certain eukaryotes but not found in humans.[6] Therefore, nitroreductases could be used to catalyze the release of antibiotic sites specifically in humans, concentrating the active drug in the place of an infection. The compound would only deliver the medicine in large amounts if an infection grows, averting the overuse of antibiotics, addressing the issue of bacteria developing antibiotic resistance, and potentially reducing or eliminating side effects from antibiotics.[7]

In spite of the antibacterial and antiparasitic properties of nitroaromatic antibiotics, drugs having nitro groups frequently evince mutagenicity and intolerable toxicity profiles, which have hampered further progress of this drug group. The potent therapeutic action of these compounds drives the search for nonmutagenic and selectively toxic nitroaromatic antibiotics that kill infectious organisms without causing harm to the host cells.[3,8,9]

Antimicrobial resistance turned out to be a remarkable threat to worldwide public health, hence bringing about fundamental demands for new drugs with better therapeutic effectiveness. In this matter, molecular hybridization is based on the combination of pharmacophoric moieties of different bioactive substances to produce a new hybrid compound with improved affinity and efficacy. In this study, we report a library of molecular hybrids composed of 2,4-dinitrobenzene attached directly to various

Received: November 12, 2021
Accepted: January 28, 2022
Published: February 7, 2022

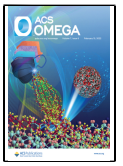

https://doi.org/10.1021/acsomega.1c06383
ACS Omega 2022, 7, 5254−5263

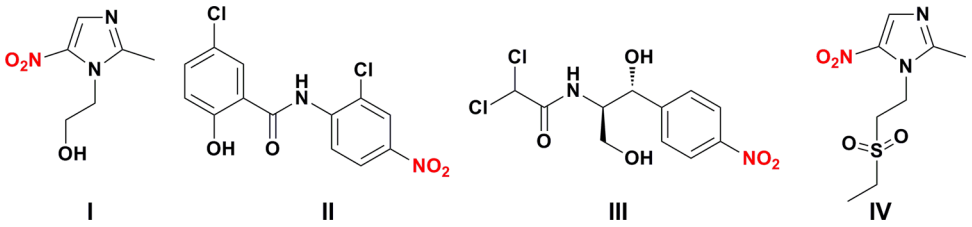

Figure 1. Structures of FDA-approved antibiotic drugs containing NO_2 groups.

Scheme 1. Synthesis of Dinitroaromatic Derivatives 3−11 *via* Sanger's Reagent

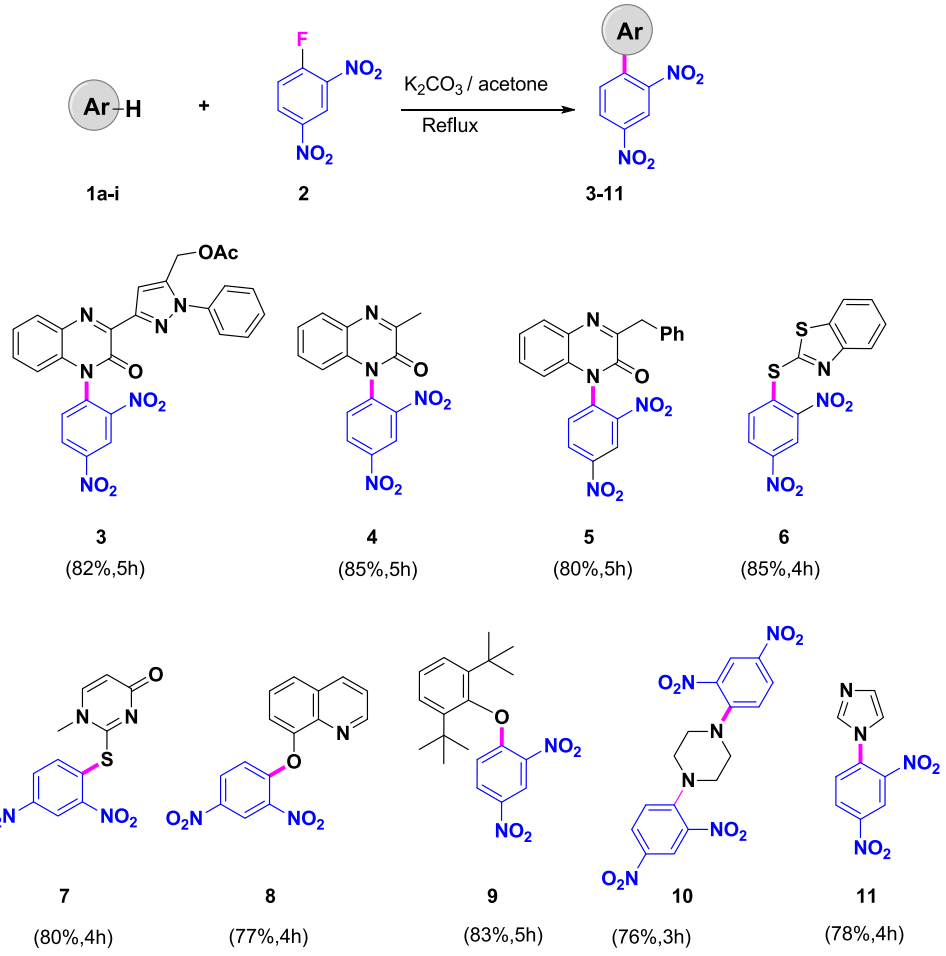

privileged scaffolds that confer desirable therapeutic potentials, e.g., imidazole,[10] piperazine,[11] methyl thiouracil,[12] substituted quinoxalinone,[13] or attached via an *O*/*S* linker to phenol,[14] 8-hydroxyquinoline,[15−17] or benzo[*d*]thiazole.[18] Minimum inhibition concentrations (MICs, μg/mL) of the nitroaromatic series were assessed against both multidrug resistant strains (MDR) and standard strains of Gram-positive (*Staphylococcus aureus* ATCC 25923) and Gram-negative (*Escherichia coli* ATCC 25922) and (*Pseudomonas aeruginosa* ATCC 29853) bacterial strains and a clinical strain of *Candida albicans*. Furthermore, molecular docking was performed to understand the binding and interactions of the promising hybrids inside the active site of the target enzyme. Sanger's reagent (1-fluoro-2,4-dinitrobenzene) was used to predict the sequence of the N-terminal of peptides by Sanger in 1945.[19] Sanger's reagent is a good reagent to synthesize smooth hybrids of organic molecules containing dinitrophenyl moieties, *via* nucleophilic aromatic substitution for the fluoride anion under mild conditions.[20]

2. RESULTS AND DISCUSSION

2.1. Chemistry. The target hybrids **3−11** were synthesized in good yields *via* nucleophilic aromatic substitution of fluoride[21−23] of the starting material 2,4-dinitrofluorobenzene with various *N*, *S*, and *O* nucleophiles **1a−i**, namely, (3-(3-oxo-3,4-dihydroquinoxalin-2-yl)-1-phenyl-1*H*-pyrazol-5-yl)-methylacetate (**1a**), 3-methylquinoxalin-2(1*H*)-one (**1b**), 3-benzylquinoxalin-2(1*H*)-one (**1c**), benzo[*d*]thiazole-2-thiol (**1d**), 1-methyl-2-thiouracil (**1e**), 8-hydroxyquinoline (**1f**), 2,6-di-*tert*-butylphenol (**1g**), piperazine (**1h**), and imidazole (**1i**), under reflux in acetone as an aprotic solvent in the presence of anhydrous K_2CO_3 to enhance nucleophilic aromatic substitutions, as shown in Scheme 1. The structures of 2,4-dinitrophenyl derivatives **3−11** were established based on their spectral data. ^{1}H NMR spectra of **3−11** showed aromatic proton signals in the following range of δ_H: 8.99−6.83 ppm. The aliphatic protons of **3−5** of Ar-CH_2/CH_3 appeared at a δ_H of

https://doi.org/10.1021/acsomega.1c06383
ACS Omega 2022, 7, 5254−5263

Table 1. Antimicrobial Activities of New Compounds (MIC μg/mL)

	Gram-positive MIC		Gram-negative MIC				fungi MIC
compds No.	*S. aureus* (ATCC 25923)	*S. aureus* clinical	*E. coli* ATCC 25922)	*E. coli* MDR	*P. aeruginosa* (ATCC 29853)	*P. aeruginosa* MDR	*C. albicans* clinical
3	>500	500	>500	**64.5**	125	125	>500
4	32.25	**16.125**	125	125	125	125	125
5	>500	500	>500	>500	125	125	>500
6	>500	500	500	>500	>500	125	500
7	**64.5**	32.25	**64.5**	125	125	125	**16.125**
8	125	125	125	125	125	125	125
9	>500	500	>500	125	125	125	>500
10	>500	>500	125	>500	>500	>500	>500
11	125	125	125	125	125	125	125
AMOX	**≤7.813**	**≤7.813**	**62.5**	**250**	**>500**	**>500**	
NYS							<2

Table 2. Cytotoxicity Data (IC_{50}, μM) of Promising Hits

compd no.	3	4	7	8	11
CC_{50} (μM)	343.72 ± 12.76	61.22 ± 1.98	120.69 ± 4.05	243.05 ± 8.43	213.28 ± 6.74

5.24, 2.02, and 4.47 ppm respectively. ^{1}H NMR of **9** and **10** showed symmetry where the di-*tert*-butyl protons in **9** appeared as a singlet signal equivalent for 18 protons at a δ_H of 1.34 ppm and also a singlet signal at a δ_H of 3.30 ppm equivalent four symmetrical CH_2 groups of the piperazine moiety of compound **10** equivalent for 8 protons. ^{13}C NMR spectra of compounds **3**−**5** showed the carbonyl of quinoxaline at δ_C values ranging at 153.4, 154.4, and 153.9 ppm, respectively. The di-*tert*-butyl carbons of **9** were detected at a δ_C of 34.6 and 30.1 ppm corresponding to quaternary carbon and methyl carbons, respectively.

2.2. Biological Evaluation. *2.2.1. MIC Determination against Various Bacteria.* The antimicrobial activity of the newly synthesized compounds was performed by microbroth dilution assay used for the determination of minimum inhibitory concentrations (MICs) according to the CLSI reference standards.[24] In this study, the MIC test was applied to assess the antibacterial properties of the target compounds **3**−**11** toward standard strains of the Gram-negative bacteria *E. coli* (ATCC 25922) and *P. aeruginosa* (ATCC 29853) and Gram-positive bacteria *S. aureus*(ATCC 25923), in addition to clinical strains of Gram-negative bacteria including *E. coli* and *P. aeruginosa* and Gram-positive bacteria *S. aureus*; also, antifungal activity against a clinical isolate of *C. albicans* using amoxicillin (AMOX) and nystatin (NYS) as antibacterial and antifungal reference standards, respectively, is evaluated as shown in Table 1.

2.2.2. SAR Study. Exceptionally, **3** exhibited a promising antibacterial result (MIC 64. 5 μg/mL) against the multidrug resistant strain of *E. coli*, which represents four times the activity of AMOX (MIC 250 μg/mL). In addition, the antimicrobial study revealed that the hybrid of 1-(2,4-dinitrophenyl)-3-methylquinoxalin-2(1*H*)one (**4**) showed at least fourfold (MIC 125 μg/mL) the antimicrobial activity of AMOX (MIC > 500 μg/mL) against both standard and clinical strains of *P. aeruginosa*. Moreover, it showed twofold (MIC 125 μg/mL) the antimicrobial activity of AMOX (MIC 250 μg/mL) against MDR *E. coli*. Also, it demonstrated less than or equal to half potency (MIC 16.125 μg/mL) of AMOX (MIC ≤ 7.8125 μg/mL) against the resistant Gram-positive strain of *S. aureus* and half potency (MIC 125 μg/mL) of AMOX (MIC 62.5 μg/mL) against the standard strain of *E. coli*. Noticeably, the other quinoxaline hybrids **3** and **5** showed similar enhanced MIC to **4** toward standard and clinical strains of *P. aeruginosa*.

Concerning the hybrid with 2-((2,4-dinitrophenyl)thio)-1-methylpyrimidin-4(1*H*)-one (**7**), it elicited approximately (MIC 64.5 μg/mL) the same MIC of AMOX (MIC 62.5 μg/mL) toward the standard strain of *E. coli*; what is more is that it elicited double the activity of AMOX against MDR *E. coli* and at least fourfold the activity of AMOX against both standard and MDR strains of *P. aeruginosa*. This hybrid was active against the clinical strain of *Candida*; it showed a moderate activity (MIC 16.125 μg/mL) compared to that of the standard antifungal drug NYS.

The hybrids 2,4-dinitrophenyl-imidazole (**11**) and 8-(2,4-dinitrophenoxy)quinoline (**8**) are equipotent toward all tested microorganisms (MIC 125 μg/mL); they displayed twofold the antibacterial activity of AMOX (MIC 250 μg/mL) against MDR *E. coli* and showed at least fourfold the potency of AMOX (MIC > 500 μg/mL) against both MDR and a standard strain of *P. aeruginosa* (ATCC 29853). A similar activity profile toward MDR *E. coli* and both MDR and a standard strain (ATCC 29853) of *P. aeruginosa* was noticed for **9**. Among all screened compounds, 2-[(2,4-dinitrophenyl)thio]benzo[*d*]thiazole (**6**) and bis(2,4-dinitrophenylpiperazine) (**10**) exhibited low antibacterial activities, as shown in Table 1.

2.2.3. In Vitro Cytotoxicity Screening Against the Human Cell Line WI-38. In order to evaluate the selective toxicity of the most active compounds **3**, **4**, **7**, **8**, and **11**, they were tested against the human diploid lung fibroblast cell line WI-38 using MTT assay,[25] as shown in Table 2 and Figure 2. Interestingly, compound **3** possessed a remarkable noncytotoxic effect on these normal WI-38 cells (CC_{50} 343.72 μM). Hence, this compound is further evaluated by *in vitro* assays as a DNA gyrase inhibitor.

2.3. Enzyme Assessment of DNA Gyrase. Compound **3** is selected, being the safest compound, for further evaluation against the bacterial DNA gyrase enzyme.

2.3.1. DNA Gyrase Supercoiling Assay. Compound **3** was screened for its ability to inhibit DNA gyrase supercoiling (using *E. coli* DNA gyrase)[26,27] using TopoGEN DNA gyrase assay kit protocol TG1003. Ciprofloxacin and novobiocin are used as

https://doi.org/10.1021/acsomega.1c06383
ACS Omega 2022, 7, 5254−5263

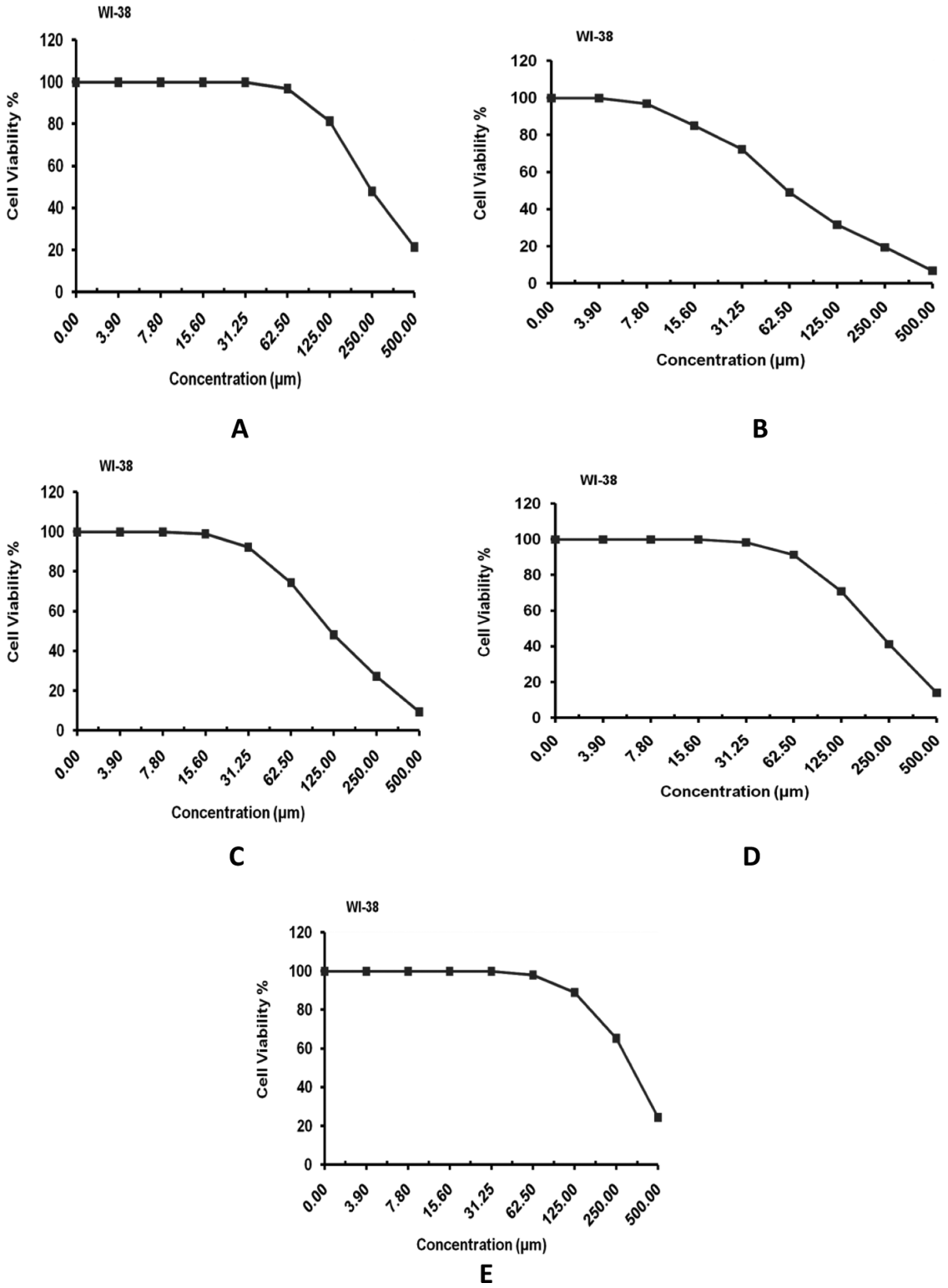

Figure 2. Cytotoxic effect of compounds **3** (A), **4** (B), **7** (C), **8** (D), and **11** (E) on the human cell line WI-38.

reference standards. The results revealed that it inhibited DNA gyrase supercoiling at the micromolar level, IC_{50} 0.869 μM, which is more than that of novobiocin (IC_{50} 1.23 μM); however, it displayed lower inhibitory activity than that of ciprofloxacin (IC_{50} 0.282 μM), as shown in Table 3.

2.3.2. DNA Gyrase ATPase Assay. Compound **3** was further tested in DNA gyrase ATPase assay using a commercially available *E. coli* DNA Gyrase ATPase assay Kit (inspiralis).[28] It

Table 3. DNA Gyrase Assays for Compound 3

	E. coli DNA gyrase IC_{50} (μM)	
compound	ATPase activity	supercoiling assay
3	0.16 ± 007	0.869 ± 0.046
ciprofloxacin		0.282 ± 0.015
novobiocin	0.09 ± 0.004	1.23 ± 0.04

https://doi.org/10.1021/acsomega.1c06383
ACS Omega 2022, 7, 5254−5263

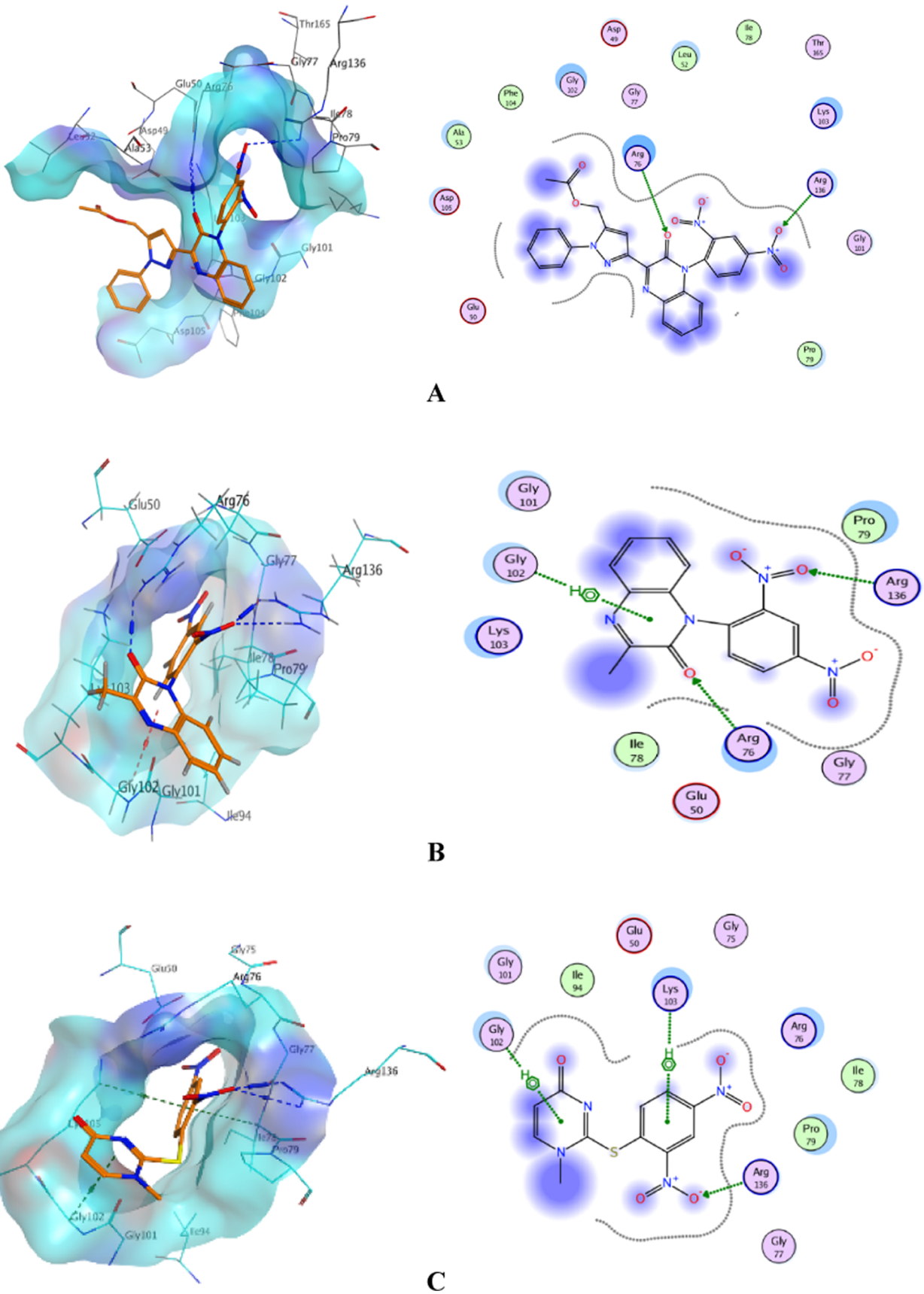

Figure 3. continued

https://doi.org/10.1021/acsomega.1c06383
ACS Omega 2022, 7, 5254−5263

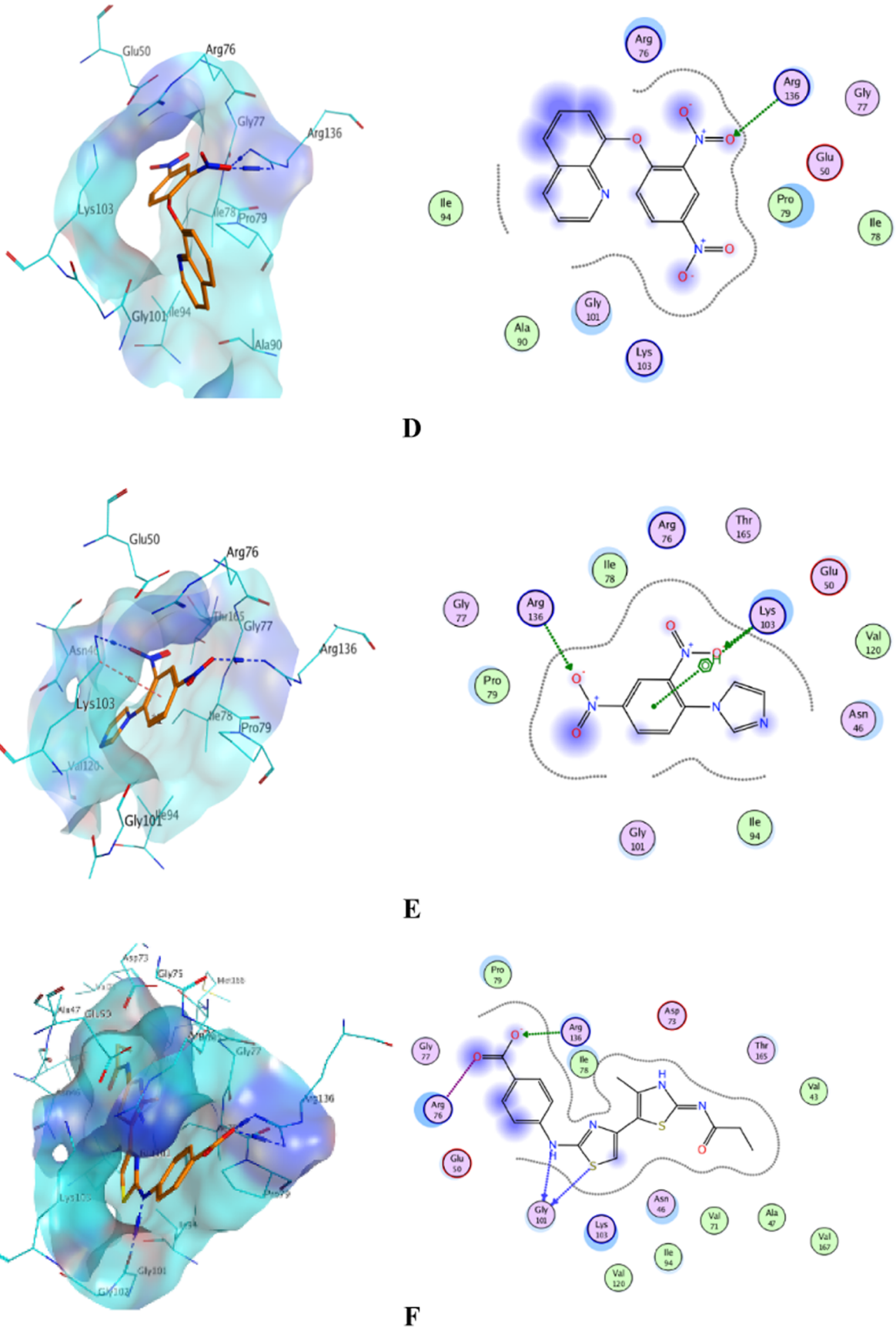

Figure 3. Proposed three-dimensional (3D) and two-dimensional (2D) binding modes of compounds **3** (A), **4** (B), **7** (C), **8** (D), **11** (E), and ligand (F).

https://doi.org/10.1021/acsomega.1c06383
ACS Omega 2022, 7, 5254−5263

inhibited the ATPase activity of DNA gyrase (IC_{50} 0.16 μM) approximately in the same range of the novobiocin reference standard (IC_{50} 0.09 μM), as shown in Table 3.

2.4. Molecular Docking Study. In recent decades, the DNA gyrase enzyme has been identified as one of the most verified and researched targets for the generation of novel antibacterial medicines.[29,30] The critical importance of DNA gyrase in bacterial survival and absence in higher eukaryotes make such an enzyme an appropriate target for developing new therapeutics in terms of selective toxicity.[31]

In this study, the preferential activity of our compounds toward Gram-negative bacteria routes us to further explore of their binding interactions by docking into the active site of DNA gyrase B.

A docking study was conducted using MOE 2014.09 software to show the possible interactions between our novel promising compounds and bacterial DNA gyrase B. Here, our target compounds **3**, **4**, **7**, **8**, and **11** were docked to the ATP binding site of *E. coli* DNA gyrase B (PDB code: 4DUH), as shown in Figure 3A–E, respectively.[32−34]

The outcome of our docking study is illustrated in Table 4 and Figures 3 and 4. The studied compounds were found to fit well in the ATP active site, with binding energies from −5.378 to −6.803 kcal/mol. Compound **4** revealed the best docking score of −6.803 kcal/mol, while the ligand exhibited a docking score of −6.712 kcal/mol. Redocking of the cocrystallized ligand revealed an RMSD value of 0.7068 A^0, indicating the validity of the used docking protocol. It showed H-bond interactions with the important amino acids Arg76, Gly101, and Arg136, as shown in Figure 3F.

Table 4. Docking Results of Compounds 3, 4, 7, 8, and 11 against *E. coli* DNA Gyrase B

compd. no.	docking score (kcal/mol)	interacting residues (type of interaction)	distance (A^0)
3	−5.923	Arg76 (H-bond)	2.68
		Arg136 (H-bond)	2.92
		Arg136 (H-bond)	2.50
4	−6.803	Arg76 (H-bond)	3.13
		Gly102 (Pi-H)	4.37
		Arg136 (H-bond)	2.89
		Arg136 (H-bond)	3.13
7	−5.378	Gly102 (Pi-H)	3.80
		Lys103 (Pi-H)	4.40
		Arg136 (H-bond)	2.62
8	−5.516	Arg136 (H-bond)	2.59
		Arg136 (H-bond)	3.02
11	−5.291	Lys103 (H-bond)	3.08
		Lys103 (Pi-H)	3.75
		Arg136 (H-bond)	3.01
ligand	−6.712	Arg76 (H-bond)	3.66
		Gly101 (H-bond)	2.93
		Gly101 (H-bond)	3.50
		Arg136 (H-bond)	3.05

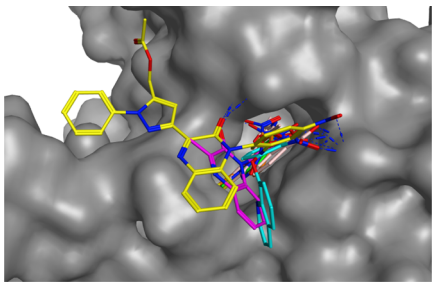

Figure 4. Overlay of the dinitrophenyl derivatives: **3** (yellow), **4** (purple), **7** (orange), **8** (cyan), **11** (green), and the cocrystallized ligand (pink) docked into the ATP binding site of DNA gyrase B.

Interestingly, in all the docked compounds **3**, **4**, **7**, **8**, and **11**, the 2,4-dinitrophenyl motif was buried in a hydrophobic cavity lined with Arg76, Ile78, and Pro79 residues. Also, one of the nitro groups of these derivatives developed hydrogen bond interactions with the crucial residue Arg136, which is known to be a critical amino acid for all ATPase inhibitors binding.[35] Concerning the 2,4-dinitrophenyl-3-methylquinoxalin-2-one (**3**) and **4**, another hydrogen bond interaction was observed between the quinoxaline-2-one oxygen atom and Arg76. Additionally, Gly102 was involved in the Pi-H interaction with the quinoxaline moiety of compound **4**. In the case of the pyrimidine derivative **7**, the dinitrophenyl moiety reacted with the active site through H-bonds with Arg136 and Pi-H interactions with Lys103. The pyrimidine ring of compound **7** was also incorporated in the binding to the active site through forming Pi-H interactions with Gly102. In the imidazole derivative **11**, the 2,4-dinitrophenyl moiety displayed the same binding pattern in which one of the nitro groups formed H-bonds with the essential Arg136 residue, while the second nitro group acted as a hydrogen bond acceptor for Lys103. Furthermore, the phenyl ring was involved in the Pi-H interaction with Lys103. On the other hand, the binding to Arg136 was the only observed H-bond interaction in the case of compound **8**.

2.5. *In Silico* Physicochemical and Pharmacokinetic Property Prediction. Swiss ADME was used to assess the physicochemical and pharmacokinetic characteristics of the promising compounds **3**, **4**, **7**, **8**, and **11**.[36,37] As shown in Table 5, compounds **4**, **7**, **8**, and **11** displayed no violations for Lipinski's rule (Log P ≤ 5, number of hydrogen bond donors ≤ 5, M_w ≤ 500, and number of hydrogen bond acceptors ≤ 10), while compound **3** revealed only one violation (M_w > 500). High-topological polar surface areas were observed for all compounds (TPSA = 109.46−170.65 A^0). All of the compounds have 3−8 rotatable bonds, suggesting structural flexibility to their biological target.

Concerning the pharmacokinetic properties of the screened compounds as shown in Table 6, it was noticed that all compounds have no BBB permeation, and consequently, they are not predictable to show CNS side effects. In addition, low gastrointestinal absorption was observed in the case of compounds **3** and **7**, while compounds **4**, **8**, and **11** displayed high GI absorption ability.

The most important element determining absorption is bioavailability that is a measure of the amount of chemical in the plasma. All of the tested compounds have high scores of bioavailability of 0.55 except compound **3** that showed a bioavailability score of 0.17. Swiss ADME also performed pan-assay interference compound screening and found no alerts for any of the compounds.

3. CONCLUSIONS

A series of hybrids containing 2,4-dinitrophenyl moieties were prepared *via* nucleophilic aromatic substitution of the fluoride anion of Sanger's reagent by various *N*, *S*, and *O* nucleophiles,

https://doi.org/10.1021/acsomega.1c06383
ACS Omega 2022, 7, 5254−5263

Table 5. *In Silico* Prediction of Physicochemical Properties of the Compounds 3, 4, 7, 8, and 11

compd no.	HBD	HBA	M_w	M log P	Lipinski's violation	TPSA	no. of rotatable bonds
3	0	9	526.12	1.73	1	170.65	8
4	0	6	326.27	0.85	0	126.53	3
7	0	6	308.27	0.09	0	151.83	4
8	0	6	311.25	1.70	0	113.76	4
11	0	5	234.17	0.12	0	109.46	3

Table 6. *In Silico* Prediction of Pharmacokinetic Properties of the Compounds 3, 4, 7, 8, and 11

compd no.	GIT absorption	BBB permeability	bioavailability score	PAINS alert
3	low	no	0.17	0
4	high	no	0.55	0
7	low	no	0.55	0
8	high	no	0.55	0
11	high	no	0.55	0

Overall, these results present compound **3** as a promising scaffold on which other molecules can be modeled to deliver new antimicrobial agents with improved potency safety and pharmacokinetic properties. The docking analysis unveiled the capability of the promising hybrid to well-accommodate the ATP binding site of *E. coli* DNA gyrase B. Moreover, *in vitro* assays proved its inhibitory activity toward DNA gyrase enzymes. ADME calculations indicated that this compound has acceptable pharmacokinetics and drug likeness properties, and the ecytotoxicity test proved the safety of this promising hit.

4. EXPERIMENTAL SECTION

All reactions were carried out in dried glassware. NMR spectra were measured using a JEOLJNM ECA 500. The deuterated solvent was used as an internal deuterium lock. ^{13}C NMR spectra were recorded using the UDEFT pulse sequence and broad band proton decoupling at 125 MHz. All chemical shifts (δ) are stated in units of parts per million (ppm) and presented using TMS as the standard reference point. CHN analyses were performed using a Flash 2000 organic elemental analyzer. Melting points were recorded using a Thermo Scientific, model no: 1002D, 220−240 V; 200 W; 50/60 Hz and are uncorrected. IR (KBr) ν_{max} (cm^{-1}) data were recorded using a Perkin Elmer; Fourier transform infrared (FT-IR) Spectrum BX; and Bruker tensor 37 FT-IR. Reaction time was monitored by TLC on Merck silica gel aluminum cards (0.2 mm thickness) with a fluorescent indicator at 254 nm. Visualization of the TLC during monitoring of the reaction was done using a UV VILBER LOURMAT 4 w-365 or 254 nm tube.

4.1. Chemistry. *4.1.1. General Method for the Synthesis of Compounds (**3**−**11**).* To a solution of aromatic nucleophiles **1a**−**i** (1.0 mmol) in dry acetone (20 mL), anhydrous potassium carbonate (2.0 mmol) was added; then, the reaction mixture was stirred under reflux for 20 min. Sanger's reagent (1.2 mmol) was added,[38] and the mixture was heated under reflux for the reported time; the reaction progress was monitored with TLC. After reaction completion, the mixture was cooled and then poured onto cold water (100 mL); the formed precipitate of the desired product was filtered, washed with water, dried, and recrystallized from ethanol to give the desired products **3**−**11**.

*4.1.2. 1-N-(2,4-Dinitro phenyl-3-[5-(acetoxymethyl)-1-Phenyl pyrazol-3-yl]quinoxalin-2-one (**3**).* Yellowish-white powder (0.43 g, 82%); R_f = 0.75 (EtOAc/*n*-hexane 1:1); m.p = 210−212 °C; **IR(KBr)**ν_{max} (cm^{-1}): 3163, 3108, 3057, 1738, 1682, 1604, 1536, 1491, 1445;**^{1}H NMR** (500 MHz, dimethyl sulfoxide (DMSO)-d_6) δ_H: 8.99 (d, J = 3.5 Hz, 1H, Ar-**H**); 8.73 (dd, J = 11.5 Hz, J = 3.5 Hz, 1H, Ar-**H**); 8.18−8.22 (m, 1H, Ar-**H**); 8.07 (d, J = 11.5 Hz, 1H, Ar-**H**); 7.78−7.84 (m, 2H, Ar-**H**); 7.49−7.73 (m, 7H, Ar-**H**); 5.24 (s, 2H, −C**H**$_2$); 2.02 (s, 3H, CO−C**H**$_3$) Figure S1; **^{13}C NMR** (125 MHz, DMSO-d_6) δ_C: 170.1, 153.4, 150.4, 146.9, 144.8, 142.1, 139.9, 139.7, 139.3, 138.5, 131.6, 130.3, 129.9, 129.6, 129.2, 128.9, 127.3, 126.9, 125.4, 125.1, 122.1, 111.9, 56.2, 20.6, Figure S2; Anal. calcd for $C_{26}H_{18}N_6O_7$: C, 59.32; H, 3.45; N, 15.96; Found C, 59.54; H, 3.38; N, 15.86

*4.1.3. 1-(2,4-Dinitrophenyl)-3-methylquinoxalin-2(1H)-one (**4**).* Colorless crystals (0.28 g, 85%); R_f = 0.675 (EtOAc/*n*-hexane 1:1); m.p = 128−130 °C; **IR(KBr)**ν_{max} (cm^{-1}): 3102, 3032, 1607, 1535, 1504, 1479;**^{1}H NMR**(500 MHz, DMSO-d_6) δ_H: 8.92 (d, J = 3.5 Hz, 1H, Ar-**H**); 8.70 (dd, J = 9.0 Hz, J = 2.5 Hz, 1H, Ar-**H**); 8.0 (d, J = 9 Hz, 2H, Ar-**H**); 7.64−7.70 (m, 2H, Ar-**H**); 7.59 (dd, J = 8.0 Hz, J = 1.5 Hz, 1H, Ar-**H**); 2.74 (s, 3H, −C**H**$_3$) Figure S3; **^{13}C NMR** (125 MHz, DMSO-d_6) δ_C: 154.4, 149.7, 147.3, 144.5, 141.8, 139.5, 137.9, 130.1, 129.9, 128.5, 128.0, 127.0, 126.8, 121.8, 20.2, Figure S4; Anal. calcd for $C_{15}H_{10}N_4O_5$: C, 55.22; H, 3.09; N, 17.17; Found C, 55.43; H, 3.15; N, 17.25.

*4.1.4. 3-Benzyl-1-(2,4-dinitrophenyl)quinoxalin-2(1H)-one (**5**).* Colorless crystals (0.33 g, 82%); R_f = 0.8 (EtOAc/*n*-hexane 1:1); m.p = 162−164 °C; **IR(KBr)**ν_{max} (cm^{-1}): 3093, 2872, 1672, 1602, 1533, 1396;**^{1}H NMR** (500 MHz, DMSO-d_6) δ_H: 8.91 (d, J = 2.5 Hz, 1H, Ar-**H**); 8.66 (dd, J = 9 Hz, J = 2.5 Hz, 1H, Ar-**H**); 8.06 (q, J = 11.0 Hz, 1H, Ar-**H**); 7.87 (d, J = 9.0 Hz, 1H, Ar-**H**); 7.70−7.73 (m, 2H,Ar-**H**); 7.64 (q, J = 9.5 Hz, 1H, Ar-**H**); 7.37 (d, J = 7.0 Hz, 2H, Ar-**H**); 7.30 (t, J = 7.5 Hz, 2H, Ar-**H**); 7.23 (t, J = 7.5 Hz, 1H, Ar-**H**); 4.47 (s, 2H, −C**H**$_2$) Figure S5; **^{13}C NMR** (125 MHz,DMSO-d_6) δ_C: 153.9, 149.4, 148.8, 144.5, 141.9, 139.5, 137.9, 136.9, 130.5, 129.8, 129.5, 128.7, 128.5, 128.3, 126.8, 126.6, 126.6, 121.7, 39.5, Figure S6; Anal. calcd for $C_{21}H_{14}N_4O_5$: C, 62.69; H, 3.51; N, 13.92; Found C, 62.33; H, 3.70; N, 13.65.

*4.1.5. 2-[(2,4-Dinitrophenyl)thio]benzo[d]thiazole (**6**).* Yellowish-white powder (0.28 g, 84%); R_f = 0.75 (EtOAc/*n*-hexane 1:1); m.p = 158−160 °C; **IR(KBr)**ν_{max} (cm^{-1}): 3107, 3067, 1597, 1530, 1454, 1413, 1347; **^{1}H NMR**(500 MHz, DMSO-d_6) δ_H: 8.89 (d, J = 2.5 Hz, 1H, Ar-**H**); 8.37 (dd, J = 8.5 Hz, J = 2.5 Hz, 1H, Ar-**H**); 8.20 (d, J = 7.5 Hz, 1H, Ar-**H**); 8.13 (d, J = 8.0 Hz, 1H, Ar-**H**); 7.63−7.53 (m, 3H, Ar-**H**) Figure S7; **^{13}C NMR** (125 MHz, DMSO-d_6) δ_C: 158.1, 153.1, 145.7, 145.0, 140.8, 137.7, 130.8, 128.4, 127.2, 126.8, 123.5, 122.8, 121.3, Figure S8; Anal. calcd for $C_{13}H_7N_3O_4S_2$: C, 46.84; H, 2.12; N, 12.61; Found C, 46.57; H, 1.99; N, 12.82

*4.1.6. 2-[(2,4-Dinitrophenyl)thio]-1-methylpyrimidin-4(1H)-one (**7**).* Pale-yellow powder (0.26 g, 84%); R_f = 0.8 (EtOAc/*n*-hexane 1:1); m.p = 118−121 °C; **IR(KBr)**ν_{max} (cm^{-1}): 3109, 3057, 2933, 2883, 1611, 1580, 1546; **^{1}H NMR** (500 MHz, DMSO-d_6) δ_H: 8.87 (d, J = 3 Hz, 1H, Ar-**H**); 8.60−

https://doi.org/10.1021/acsomega.1c06383
ACS Omega 2022, 7, 5254−5263

8.64 (m, 2H, Ar-**H**); 7.88 (d, J = 8.5 Hz, 1H, Ar-**H**); 7.07 (d, J = 6 Hz, 1H, Ar-**H**); 2.24 (s, 3H, $-CH_3$), Figure S9. **^{13}C NMR** (125 MHz, DMSO-d_6) δ_C: 171.5, 166.6, 160.4, 148.5, 144.8, 141.8, 129.8, 126.8, 121.6, 103.8, 13.4, Figure S10; Anal. calcd for $C_{11}H_8N_4O_5S$: C, 42.86; H, 2.62; N, 18.17, Figure S10; Found C, 42.93; H, 2.68; N, 18.02.

*4.1.7. 8-(2,4-Dinitrophenoxy)quinoline (**8**).* Yellowish-white powder (0.24 g, 77%); R_f = 0.5 (EtOAc/*n*-hexane 1:1); m.p = 160−162 °C; **IR(KBr)**ν_{max} (cm^{-1}): 3103, 3060, 3005, 1605, 1529, 1472; **^{1}H NMR**(500 MHz, DMSO-d_6)δ_H:8.91 (d, J = 2.5 Hz, 1H, Ar-**H**); 8.81 (t, J = 2.25 Hz, 1H, Ar-**H**); 8.52 (d, J = 7.5 Hz, 1H, Ar-**H**); 8.25 (q, J = 12Hz,1H, Ar-**H**); 8.06 (d, J = 8 Hz, 1H, Ar-**H**); 7.82 (d, J = 7 Hz, 1H, Ar-**H**); 7.74 (t, J = 7.5 Hz, 1H, Ar-**H**); 7.62 (q, J = 13 Hz, 1H, Ar-**H**); 6.83 (d, J = 10 Hz, 1H, Ar-**H**), Figure S11; **^{13}C NMR** (125 MHz, DMSOd_6) δ_C: 156.2, 151.1, 148.1, 140.9, 139.7, 138.1, 136.7, 129.9, 129.3, 127.1, 127.0, 122.6, 121.9, 121.6, 118.4, Figure S12; Anal. calcd for $C_{15}H_9N_3O_5$: C, 57.88; H, 2.91; N, 13.50; Found C, 57.53; H, 3.12; N, 13.77

*4.1.8. 1,3-Di-tert-butyl-2-(2,4-dinitrophenoxy)benzene (**9**).* Pale-yellow powder (0.31 g, 83%); R_f = 0.35 (EtOAc/*n*-hexane 1:1); m.p = 137−140 °C; **IR(KBr)**ν_{max} (cm^{-1}): 3100, 2964, 1604, 1533, 1476, 1431; **^{1}H NMR**(500 MHz, DMSO-d_6) δ_H: 8.72 (d, J = 2.5 Hz,1H, Ar-H); 8.43 (dd, J = 8 Hz, J = 2.5 Hz, 1H, Ar-H); 7.88 (d, J = 8 Hz, 1H,Ar-H); 7.49 (s, 1H, Ar-H); 7.11 (s, 2H, Ar-H); 1.34 (s, 18H, *t*-Bu-H) Figure S13; **^{13}C NMR** (125 MHz, DMSO-d_6) δ_C: 155.5, 148.8, 145.9, 141.0, 139.7, 132.9, 126.6, 125.6, 124.4, 119.4, 34.6, 30.1, Figure S14; Anal. calcd for $C_{20}H_{24}N_2O_5$: C, 64.50; H, 6.50; N, 7.52; Found C, 64.71; H, 6.68; N, 7.80.

*4.1.9. 1,4-bis(2,4-Dinitrophenyl)piperazine (**10**).* Off-white powder (0.32 g, 76%); R_f = 0.7 (EtOAc/*n*-hexane 1:1); m.p = 260−262 °C; **IR(KBr)**ν_{max} (cm^{-1}): 3079, 3008, 2919, 2880, 1598, 1533, 1500, 1444;**^{1}H NMR** (500 MHz, DMSO-d_6) δ_H: 8.61 (d, J = 2.5 Hz, 2H, Ar-H); 8.27 (dd, J = 9.5 Hz, J = 2.5 Hz, 2H, Ar-H); 7.31 (d, J = 10 Hz, 2H, Ar-H); 3.30 (s, 8H, piprazine-H), Figure S15; **^{13}C NMR** (125 MHz, DMSO-d_6) δ_C: 148.2, 136.4, 135.5, 128.0, 123.7, 118.5, 47.9, Figure S16; Anal. calcd for $C_{16}H_{14}N_6O_6$: C, 45.94; H, 3.37; N, 20.09; Found C, 46.11; H, 3.48; N, 20.26

*4.1.10. 1-(2,4-Dinitrophenyl)-1H-imidazole (**11**).* Off-white powder (0.18 g, 77%); R_f = 0.35 (EtOAc/*n*-hexane 1:1); m.p = 110−112 °C; **IR(KBr)**ν_{max} (cm^{-1}): 3152, 3121, 3063, 1607, 1532, 1416, 1349; **^{1}H NMR**(500 MHz, DMSO-d_6) δ_H: 8.91 (d, J = 2 Hz, 1H, Ar-**H**); 8.63 (dd, J = 9 Hz, J = 2.5 Hz, 1H, Ar-**H**); 7.98 (dd, J = 7.5 Hz, J = 1.5 Hz, 2H, Ar-**H**); 7.49 (s, 1H, Ar-**H**); 7.12 (s, 1H, imidazole-H), Figure S17; **^{13}C NMR** (125 MHz, DMSO-d_6 δ_C: 146.4, 143.8, 137.5, 134.9, 130.2, 129.8, 128.7, 121.3, 120.4, Figure S18; Anal. calcd for $C_9H_6N_4O_4$: C, 46.16; H, 2.58; N, 23.93; Found C, 46.34; H, 2.42; N, 24.08

The experimental parts of MIC, *in vitro* cytotoxcity, and enzymatic assay are submitted in the Supporting Information.

4.2. Docking Studies. Molecular Operating Environment software (MOE 2014.09) was used for the docking investigation. The builder button was used to create structures for **3**, **4**, **7**, **8**, and **11**. The standard MMFF94x force field was then used to reduce the energy of the drawn chemicals. The investigated compounds were docked into the DNA gyrase B binding site (PDB: 4DUH).The water molecules were removed during the docking process. The missing hydrogen atoms were added in order to give the right ionization states to the protein structure. MOE's "Docking" module was used to generate molecular docking. With the default settings, the docking process was carried out. The best 30 poses were scored using the GBVI/WSA dG (GeneralizedBorn Volume Integral/Weighted Surface Area) grading algorithm. The MOE tool "Ligand Interactions" was now used to analyze the docking data by displaying the protein−ligand interactions in the complex's active region.

■ ASSOCIATED CONTENT

Supporting Information

The Supporting Information is available free of charge at https://pubs.acs.org/doi/10.1021/acsomega.1c06383.

Copy of ^{1}H NMR and ^{13}C NMR of all synthesized compounds (PDF)

■ AUTHOR INFORMATION

Corresponding Author

Mohammed Salah Ayoup − *Department of Chemistry, Faculty of Science, Alexandria University, 21525 Alexandria, Egypt;* orcid.org/0000-0001-6715-5478; Email: mohammedsalahayoup@gmail.com, mohamed.salah@alexu.edu.eg

Authors

Ahmed R. Rabee − *Department of Chemistry, Faculty of Science, Alexandria University, 21525 Alexandria, Egypt*

Hamida Abdel-Hamid − *Department of Chemistry, Faculty of Science, Alexandria University, 21525 Alexandria, Egypt*

Marwa F. Harras − *Department of Pharmaceutical Medicinal Chemistry, Faculty of Pharmacy (Girls), Al-Azhar University, Cairo 11651, Egypt*

Nagwan G. El Menofy − *Department of Microbiology and Immunology, Faculty of Pharmacy (Girls), Al-Azhar University, Cairo 11651, Egypt*

Magda M. F. Ismail − *Department of Pharmaceutical Medicinal Chemistry, Faculty of Pharmacy (Girls), Al-Azhar University, Cairo 11651, Egypt*

Complete contact information is available at: https://pubs.acs.org/10.1021/acsomega.1c06383

Notes

The authors declare no competing financial interest.

■ ACKNOWLEDGMENTS

The authors gratefully thank Alexandria University and Al-Azhar University for support.

■ REFERENCES

(1) Kannigadu, C.; N'Da, D. Recent advances in nitroaromatics: The synthesis and development of anti-infective drugs. *Curr. Pharm. Des.* **2020**, *26*, 1−17.

(2) Butler, M. S.; Blaskovich, M. A.; Cooper, M. A. Antibiotics in the clinical pipeline in 2013. *J. Antibiot.* **2013**, *66*, 571−591.

(3) Rice, A. M.; Long, Y.; King, S. B. Nitroaromatic Antibiotics as Nitrogen Oxide Sources. *Biomolecules* **2021**, *11*, No. 267.

(4) Huttner, A.; Verhaegh, E. M.; Harbarth, S.; Muller, A. E.; Theuretzbacher, U.; Mouton, J. W. Nitrofurantoin revisited: a systematic review and meta-analysis of controlled trials. *J. Antimicrob. Chemother.* **2015**, *70*, 2456−2464.

(5) Olender, D.; Żwawiak, J.; Zaprutko, L. Multidirectional Efficacy of Biologically Active Nitro Compounds Included in Medicines. *Pharmaceuticals* **2018**, *11*, No. 54.

(6) de Oliveira, I. M.; Henriques, J. A. P.; Bonatto, D. Insilico identification of a new group of specific bacterial and fungal

nitroreductases-like proteins. *Biochem. Biophys. Res. Commun.* **2007**, *355*, 919−925.
(7) Hibbard, H. A. J.; Reynolds, M. M. Synthesis of novel nitroreductase enzyme-activated nitric oxide prodrugs to site-specifically kill bacteria. *Bioorg. Chem.* **2019**, *93*, No. 103318.
(8) Patterson, S.; Wyllie, S. Nitro drugs for the treatment of trypanosomatid diseases: past, present, and future prospects. *Trends Parasitol.* **2014**, *30*, 289−298.
(9) Strauss, M. J. TheNitroaromatic Group in Drug Design. Pharmacology and Toxicology (for Nonpharmacologists). *Ind. Eng. Chem. Prod. Res. Dev.* **1979**, *18*, 158−166.
(10) Valls, A.; Andreu, J. J.; Falomir, E.; Luis, S. V.; Atrián-Blasco, E.; Mitchell, S. G.; Altava, B. Imidazole and Imidazolium Antibacterial Drugs Derived from Amino Acids. *Pharmaceuticals* **2020**, *13*, No. 482.
(11) Patil, M.; NoonikaraPoyil, A.; Joshi, S. D.; Patil, S. A.; Patil, S. A.; Bugarin, A. Design, synthesis, and molecular docking study of new piperazine derivative as potential antimicrobial agents. *Bioorg. Chem.* **2019**, *92*, No. 103217.
(12) Cui, P.; Li, X.; Zhu, M.; Wang, B.; Liu, J.; Chen, H. Design, synthesis and antimicrobial activities of thiouracil derivatives containing triazolo-thiadiazole as SecA inhibitors. *Eur. J. Med. Chem.* **2017**, *127*, 159−165.
(13) Ali, M. M.; Ismail, M. M. F.; El-Gaby, M. S. A.; Zahran, M. A.; Ammar, Y. A. Synthesis and Antimicrobial Activities of Some Novel Quinoxalinone Derivatives. *Molecules* **2000**, *5*, 864−873.
(14) Aissaoui, N.; Mahjoubi, M.; Nas, F.; Mghirbi, O.; Arab, M.; Souissi, Y.; Hoceini, A.; Masmoudi, A. S.; Mosbah, A.; Cherif, A.; Klouche-Khelil, N. Antibacterial Potential of 2,4-Di-tert-Butylphenol and Calixarene-Based Prodrugs from Thermophilic Bacillus licheniformis Isolated in Algerian Hot Spring. *Geomicrobiol. J.* **2019**, *36*, 53−62.
(15) Awolade, P.; Cele, N.; Kerru, N.; Singh, P. Synthesis, antimicrobial evaluation, and in silico studies of quinoline-1H-1, 2, 3-triazole molecular hybrids. *Mol. Diversity* **2020**, 2201−2218.
(16) Xu, H.; Chen, W.; Zhan, P.; Liu, X.; et al. 8-Hydroxyquinoline: A privileged structure with a broad-ranging pharmacological potential. *Med. Chem. Commun.* **2015**, *6*, 61−74.
(17) Oliveri, V.; Vecchio, G. 8-Hydroxyquinolines in medicinal chemistry: A structural perspective. *Eur. J. Med. Chem.* **2016**, *120*, 252−274.
(18) Ismail, M. M. F.; Abdulwahab, H. G.; Nossier, E. S.; El Menofy, N. G.; Abdelkhalek, B. A. Synthesis of novel 2-aminobenzothiazole derivatives as potential antimicrobial agents with dual DNA gyrase/topoisomerase IV inhibition. *Bioorg. Chem.* **2020**, *94*, No. 103437.
(19) Sanger, F. The free amino groups of insulin. *Biochem. J.* **1945**, *39*, 507−515.
(20) Smith, P. W. G.; Tatchell, A. R., *Aromatic Chemistry: Organic Chemistry for General Degree Students*; Elsevier, 2016.
(21) Ismail, M. M. F.; El-Sehrawi, H.; Elzahabi, H. S.; Shawer, T.; Ammar, Y. A. Synthesis and Antitumor Activity of Novel Hybrids of Pyrimidine/Benzimidazole Scaffolds. *Polycyclic Aromat. Compd.* **2020**, *7*, 1−15.
(22) Dolzhenko, A. V.; Chui, W. K.; Dolzhenko, A. V. Synthesis of ethyl 6-aryl-4-oxo-4, 6-dihydro-1 (12)(13) h-pyrimido-[2′, 1′: 4, 5][1, 3, 5] triazino [1, 2-a] benzimidazole-3-carboxylates. *J. Heterocycl. Chem.* **2006**, *43*, 1513−1521.
(23) Martin, D.; et al. Cyansaeureester. XXXI: Umsetzungen von 2-Guanidino-Benzimidazol MIT Elektrophilen Reagentien. *J. Prakt. Chem.* **1981**, *323*, 303−310.
(24) Weinstein, M. P.; Patel, J. B.; Burnhman, C. A.; Zimmer, B. L. Clinical and laboratory standards institute methods for dilution antimicrobial susceptibility tests for bacteria that grow aerobically standard, approval CDM-A. *M07 Methods Dilution Antimicrob Susceptibility Tests Bact That Grow Aerob*, 2018, *91*.
(25) Van Meerloo, J.; Kaspers, G. J.; Cloos, J. Cell sensitivity assays: the MTT assay. *Methods Mol. Biol.* **2011**, *731*, 237−245.
(26) Maxwell, A.; Burton, N. P.; O'Hagan, N. High-throughput assays for DNA gyrase and other topoisomerases. *Nucleic Acids Res.* **2006**, *34*, e104.
(27) Jakopin, Ž.; Ilaš, J.; Barančoková, M.; Brvar, M.; Tammela, P.; Dolenc, M. S.; Tomašič, T.; Kikelj, D. Discovery of substituted oxadiazoles as a novel scaffold for DNA gyrase inhibitors. *Eur. J. Med. Chem.* **2017**, *130*, 171−184.
(28) Gjorgjieva, M.; Tomašič, T.; Barančokova, M.; Katsamakas, S.; Ilaš, J.; Tammela, Pi.; Peterlin Mašič, L.; Kikelj, D. Discovery of benzothiazole scaffold-based DNA gyrase B inhibitors. *J. Med. Chem.* **2016**, *59*, 8941−8954.
(29) Brvar, M.; Perdih, A.; Oblak, M.; Mašič, L. P.; Solmajer, T. Insilico discovery of 2-amino-4-(2, 4-dihydroxyphenyl) thiazoles as novel inhibitors of DNA gyrase B. *Bioorg. Med. Chem. Lett.* **2010**, *20*, 958−962.
(30) Tomašić, T.; PeterlinMasic, L. Prospects for developing new antibacterials targeting bacterial type IIA topoisomerases. *Curr. Top. Med. Chem.* **2013**, *14*, 130−151.
(31) Collin, F.; Karkare, S.; Maxwell, A. Exploiting bacterial DNA gyrase as a drug target: current state and perspectives. *Appl. Microbiol. Biotechnol.* **2011**, *92*, 479−497.
(32) Bisacchi, G. S.; Manchester, J. I. A new-class antibacterial almost. Lessons in drug discovery and development: A critical analysis of more than 50 years of effort toward ATPase inhibitors of DNA gyrase and topoisomerase IV. *ACS Infect. Dis.* **2015**, *1*, 4−41.
(33) Ayoup, M. S.; Ahmed, H. E. A.; El Massry, A. M.; Senior, S.; Khattab, S. N.; Hassan, S. Y.; Amer, A. Synthesis, Docking, and Evaluation of Antimicrobial Activity of a New Series of Acyclo C-Nucleosides of 1, 2, 4-Triazolo[4, 3-a]quinoxaline Derivatives. *J. Heterocycl. Chem.* **2016**, *53*, 153−163.
(34) Amer, A.; Ayoup, M. S.; Khattab, S. N.; Hassan, S. Y.; Langer, V.; Senior, S.; Massry, A. M. E. A regio- and stereo-controlled approach to triazoloquinoxalinyl C-nucleosides. *Carbohydr. Res.* **2010**, *345*, 2474−2484.
(35) Brvar, M.; Perdih, A.; Renko, M.; Anderluh, G.; Turk, D. a.; Solmajer, T. Structure-based discovery of substituted 4, 5′-bithiazoles as novel DNA gyrase inhibitors. *J. Med. Chem.* **2012**, *55*, 6413−6426.
(36) Daina, A.; Michielin, O.; Zoete, V. SwissADME: a free web tool to evaluate pharmacokinetics, drug-likeness and medicinal chemistry friendliness of small molecules. *Sci. Rep.* **2017**, *7*, No. 42717.
(37) Ayoup, M. S.; Soliman, S. M.; Haukka, M.; Harras, M. F.; Menofy, N. G. E.; Ismail, M. M. F. Prodrugs of sulfacetamide: Synthesis, X-ray structure, Hirshfeld analysis, antibacterial assessment, and docking studies. *J. Mol. Struct.* **2022**, *1251*, No. 132017.
(38) Ayoup, M. S.; Abu-Serie, M. M.; Awad, L. F.; Teleb, M.; Ragab, H. M.; Amer, A. Halting colorectal cancer metastasis via novel dual nanomolar MMP-9/MAO-A quinoxaline-based inhibitors; design, synthesis, and evaluation. *Eur. J. Med. Chem.* **2021**, *222*, No. 113558.

https://doi.org/10.1021/acsomega.1c06383
ACS Omega 2022, 7, 5254−5263